PERGAMON

International Journal of Solids and Structures 40 (2003) 2999–3020

INTERNATIONAL JOURNAL OF SOLIDS and STRUCTURES

www.elsevier.com/locate/ijsolstr

# Enhancing the optimization of material distributions in composite structures using gradient architectures

Harishbabu Surendranath, Hugh A. Bruck *, Swami Gowrisankaran

*Department of Mechanical Engineering, University of Maryland, College Park, MD 20742, USA*

Received 29 July 2002; received in revised form 20 January 2003

**Abstract**

Many structural components encounter service conditions and hence, material performance requirements, which vary from location to location within the component resulting in a composite structure. It has been shown that abrupt transitions in material properties within a composite structure can cause concentrations of deformation, which are mitigated by gradually varying the microstructure and/or composition of materials in a gradient architecture. Structural optimization techniques, such as the homogenization method, have yet to take full advantage of gradient architectures. Many of these structural optimization techniques employ robust mathematical techniques, such as genetic algorithms (GAs), with finite element simulations to optimize material distributions in composite structures through computationally intensive stochastic, global explorations of the design search space defined by a multitude of design variables associated with the discrete representation of the composite structure. Using gradient architectures, it is demonstrated that GAs can be enhanced for composite structures by constraining the design search space through a reduction in the number of design variables, thereby substantially reducing the computational effort. For more complex material distributions, a "material gradient optimization method" is proposed that produces multiple gradient architecture constraints with more optimal solutions than obtained without using these constraints, but whose uniqueness will be dependent upon the number of layers used in the finite element simulations.


*Keywords:* Homogenization design method; Genetic algorithm; Gradient architecture; Composite structures; Finite element analysis

## 1. Introduction

Structures are often designed with material performance requirements that vary from location to location within a structure due to the service conditions. A classic example is a knife, where a hard material is required at the edge of the knife to optimize wear resistance and a tough material is required in the interior to optimize fracture resistance. It is difficult to find a single material that satisfies all of the requirements, since properties such as toughness and hardness are inversely related. Therefore, a distribution of materials with associated properties that match the variation in material performance requirements will be selected,

* Corresponding author. Fax: +1-301-314-9477.
*E-mail address:* bruck@eng.umd.edu (H.A. Bruck).

0020-7683/03/$ - see front matter © 2003 Published by Elsevier Science Ltd.
doi:10.1016/S0020-7683(03)00090-8

resulting in a composite structure. In many cases, concentrations of deformation arise due to abrupt transitions in the material properties. By gradually varying the volume fraction and/or microstructure of the materials throughout a structure, a composite structure can be fabricated with a gradient architecture that mitigates these deformations, optimizing material performance. This concept was first suggested by Bever and Duwez (1972), and its exploitation in a variety of composite structures has been extensively investigated, predominantly in the United States and Japan within the past decade (Niino and Maeda, 1990; Markworth et al., 1995; Goettler et al., 1997; Suresh and Mortenson, 1998).

Effective and efficient algorithms are needed that can determine the material distribution in a composite structure to optimize a given material performance requirement. The homogenization design method has been demonstrated as a powerful analysis tool that can be used directly to predict the property-structure relationships of many existing classes of composites and to design the topological macrostructure of a new generation of composites so as to optimize their mechanical properties (Bendsoe and Kikuchi, 1988; Takano et al., 1998). The homogenization design method assumes a certain type of microstructure for the material to determine the effective properties for a given volume fraction of constituents. A well-recognized issue with the homogenization design method is the associated computational expense escalates rapidly with mesh refinement due to an increase in the number of design variables representing the volume fractions of constituents at each point within a structure, thus providing a potential obstacle to usage of the method for determining complex material distributions when searching over the complete design space (Swan and Kosaka, 1997). Therefore, more efficient methods for finding out the optimal material distribution are required that can describe complex material distributions using fewer design variables.

In a variety biological structures, from insect wings to bamboo, evidence can be found that gradient architectures have been selected through natural evolution to optimize complex material distributions, as was suggested by Bever and Duwez for synthetic composite structures (Kreuz et al., 2001; Amada et al., 1997). Using gradient architectures, complex material distributions will be described with just a few design variables determined by the gradient description. Therefore, in this investigation the formulation of the design optimization problem is modified to exploit gradient architectures for improving computational efficiency over the conventional homogenization methods by reducing the number of design variables. To demonstrate its efficacy, a genetic algorithm (GA) with and without a gradient architectural constraint is used to optimize a metal-ceramic composite disk subjected to a thermal gradient, e.g. a Thermal Barrier Coating, that is modeled using an experimentally verified 3-D thermomechanical finite element simulation approach. Such an optimization problem for composite structures has been the subject of a number of recent computational investigations (Sadagopan and Pitchumani, 1998; Ootao et al., 1999; Shimojima et al., 1999; Nadeau and Ferrari, 1999; Takaka et al., 1993; Finot et al., 1994). In the investigation conducted here, target service temperatures for the hot surface will be on the order of 1000 K, creating an extremely hot, oxidizing environment that is best resisted by a refractory material such as the ceramic, alumina. Near the cold surface, on the order of 300 K, a strong, tough and thermally conductive material such as nickel is desired. Composite structures with gradient architectures consisting of nickel and alumina have been fabricated using a variety of processes, including powder metallurgy, chemical or physical vapor deposition, and plasma spraying (Suresh and Mortenson, 1998). The difference in thermal expansion between these two materials will cause a composite structure to warp under the temperature gradient. Therefore, the focus of optimizing the structure in this investigation will be to minimize this distortion.

## 2. Design optimization problem

To optimize the design of a composite structure, it is first necessary to define the design optimization problem. In this investigation, the design problem defined using the conventional homogenization method

is compared with a modification of the design optimization problem using gradient architecture concepts. These two approaches are defined respectively as:

(1) no constraints on the nature of the material distribution in the structure (conventional homogenization method),
(2) a gradient architecture described by a one-dimensional power law (modified design optimization problem).

Though the problem formulation for the two approaches are similar, there are some subtle differences. The second approach is a lot simpler than the first and the number of design variables can be drastically reduced. Both the approaches are described in detail in the following sections.

### 2.1. No constraints on the material distribution

When the mechanical response of the body subjected to the analysis is totally unknown, constraints on the nature of the material distribution cannot be placed. In such instances, the structure has to be discretized into small elements and the material constitution of each element has to be determined. Fig. 1 shows the discrete representation of a two-dimensional body under the influence of a set of arbitrary forces and boundary conditions. The structure is made of a composite material, in which the constitution of the two components can vary with position. It is desirable to find the distribution of the two components in the structure to minimize a user-specified objective. This problem can be formulated as follows:

(1) *Design variables*: Design variables are a set of system variables, which control the response of the system, thereby controlling the objective. In this approach, the design variables are the composition of both the components at each point inside the body. If the body is considered as a continuum, infinitely many design variables are to be considered. A scheme has to be developed to reduce the number of design variables to a finite number. One way of doing this is to discretely represent the continuum by a finite number of elements, as in the finite element method. Each element or group of elements has a fixed material composition, as described in Fig. 2. There is no variation in the composition of the material inside an element. Therefore, the design variables are the design variables are $f_1^i$ and $f_2^i$, where $f_1^i$ and $f_2^i$ are the volume fractions of component 1 and 2 respectively in the $i$th element. Taking all of the design variables for a composite structure, a design vector, $\bar{f}$, can be constructed that will represent the material distribution in the design problem that it is desirable to optimize.

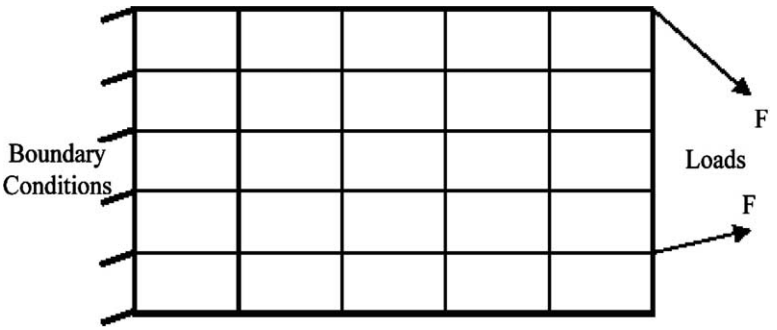


Fig. 1. Typical discrete representation of a two-dimensional body subjected to arbitrary forces and boundary conditions in the design optimization problem, where the material composition in each element is to be determined.

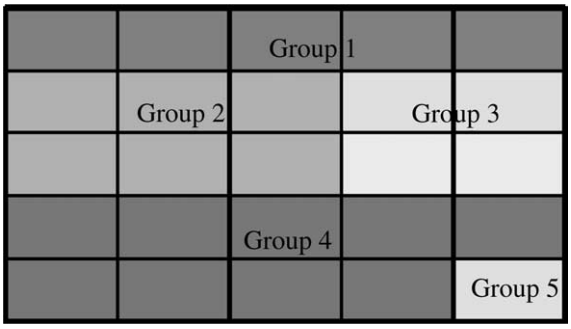


Fig. 2. Groups of elements in the discretized structure of Fig. 1 with gray-level representation of the relative material distributions between groups.

(2) *Objective function*: A mathematical description of the user-defined objective, known as the objective function, must be constructed as a scalar function of the response variables for the system (e.g., stress, strain, displacements, reaction forces) as described below:

$$G = f(\sigma, \varepsilon, u, R), \tag{1}$$

where $G$ is the objective function, $\sigma$ is the stress field, $\varepsilon$ is the strain field, $u$ is the displacement field, and $R$ is the reaction forces acting on the body. The response variables themselves are functions of the design vector, as follows:

$$[\sigma, \varepsilon, u, R] = g(\bar{f}). \tag{2}$$

It is difficult to relate the design variables and the objective function explicitly. Although the exact analytical relationship between the objective function and the design variables can be determined for simple cases, it cannot be done for the vast majority of cases. Non-linearity in the geometry, boundary conditions and material behavior in most of the real world applications makes it impossible to derive an analytical relationship between the design variables and the objective function. In such instances, the response of the objective function to a given set of design variables have to be obtained numerically. This makes it difficult to predict the nature of the objective function, its convexity and the local optima present on the objective function surface.

(3) *Constraints*: The design variables are the volume fractions of the two components. There are two main constraints that the design variables must satisfy. Assuming that the composite material under consideration comprises of only two materials, and the structure has $N$ number of groups, the constraints can be formulated in the following manner:

$$0 \leqslant f_1^i, f_2^i \leqslant 1 \quad (i = 1, \ldots, N), \tag{3a}$$

$$f_1^i + f_2^i = 1 \quad (i = 1, \ldots, N). \tag{3b}$$

From the first constraint, it can be inferred that the lower bound of the volume fraction of a component is zero. This refers to a state where the volume of the group contains only the other component. The upper bound of the volume fraction is unity. This refers to a state where the volume of the group consists only this specific component. Also, the summation of the volume fractions of the two components in a group has to be unity. This is formulated in the second constraint, which reduces the number of design variables in half.

### 2.2. One-dimensional gradient architecture constraint

In the previous approach, no constraints were placed on the nature of the material distribution in the body. In this approach, the concept of one-dimensional gradient architecture constraint is used to enhance the design problem for the same objective function by formulating new design variables and constraints as follows:

(1) *Design variables*: Fig. 3 shows the one-dimensional architecture of a simple body with one-dimensional gradient architecture. The design parameters for this architecture are $x_0$, $t$ and $p$. $x_0$ is the distance till which the body contains only component 1. The portion of the body from $x^* = x_0$ to $x^* = x_0 + t$, is the gradient transition layer and contains both the components. The design variables can be expressed as a design vector, $\bar{d}$ as described below:

$$\bar{d} = \{x_0, t, p\}. \tag{4}$$

The composition of the composite material at a distance $x$ from the start of the gradient layer, in the graded region is continuously described by a power law, given by:

$$f_2 = \left(\frac{x}{t}\right)^p, \tag{5}$$

where $f_1$ and $f_2$ are the volume fractions of component 1 and 2 respectively. $x$ is the distance from the interface and $t$ is the thickness of the gradient layer. The parameter $p$ is called the gradient exponent with values $0 \leqslant p < \infty$. From $x^* = x_0 + t$ to $x^* = L$, the composite consists only of component 2. The three parameters $x_0$, $t$ and $p$ can uniquely determine the material distribution in the body, which determines the mechanical behavior of the system under the given set of working conditions. These parameters are the design variables for this system.

For a discrete composition variation, as is the case when the composite structure is discretized into a finite number of elements, the average volume fraction for the second component of a two-phase composite in a 1-D architecture is determined as follows:

$$\overline{f_2} = \frac{1}{(x_2 - x_1)} \int_{x_1}^{x_2} \left(\frac{x}{t}\right)^p \mathrm{d}x, \tag{6}$$

Integrating the expression within the limits, the average volume fractions of the components are obtained as:

$$\overline{f_2} = \frac{1}{(x_2 - x_1)} \cdot \frac{1}{(p+1)} \cdot \frac{x_2^{p+1} - x_1^{p+1}}{t^p}. \tag{7}$$

These average volume fractions are used to determine the effective material properties of within the layer.


Fig. 3. Discretized structure with a gradient architecture described using a one-dimensional power law, $f_2 = [(x^* - x_0)/t]^p$ for $x_0 < x^* < x_0 + t$.

(2) *Constraints*: The design variables are geometric in nature. The type of constraints on these variables differs in nature from the constraints in the previous approach, where the design variables were the volume fractions. The constraints on the design variables in this approach are:

$$0 \leqslant x_0 \leqslant L, \tag{8a}$$

$$0 \leqslant t \leqslant L, \tag{8b}$$

$$0 \leqslant (x_0 + t) \leqslant L, \tag{8c}$$

$$0 < p < \infty. \tag{8d}$$

The first constraint bounds the range of values of the variable $x_0$. The lower and upper bounds for $x_0$ is zero and $L$ respectively. These correspond to two extreme conditions: the first one being the case where there is no layer of pure component 1 in the body, and the second corresponding to a state where the entire composition of the body comprises of only component 1. The second constraint restricts the range of values the parameter $t$ can assume. The value $t = 0$ corresponds to the state where there is no graded interlayer. The value $t = L$ corresponds to the state where the graded layer occupies the whole dimension of the body. Both $x$ and $t$ are non-negative. This assures the non-negativity of the volume fraction of component 2 from Eq. (5). The constraint $(x_0 + t) \leqslant L$ assures that the combined thickness of the layer with only component 1 and the gradient layer does not exceed the total thickness of the whole structure. The constraint $p > 0$ assures from Eq. (5) that the value of the volume fraction is less than unity throughout the graded layer. The value $p = 0$ was not included to avoid the redundancy in sampling of the design space that produces a bimaterial distribution identical to $t = 0$, as illustrated in Fig. 4.

### 2.3. Genetic algorithm optimization method

To optimize the design problem, a random, stochastic, global search optimization method known as the GA was employed. The GA is a biologically inspired optimization method that evolves optimal solutions using genetic concepts. There are two main reasons behind choosing a GA as the optimization method for this specific problem rather than alternative gradient-based techniques. They are:

(a) The nature of the objective function might contain multiple minima, in which case, gradient methods might get caught in one of the local optima, failing to determine the global optimum.
(b) The computation of gradients can be computationally intensive or numerically unstable because of the large number of design variables.

In the GA, an initial population of random guesses for a set of design parameters is generated in a matrix, $D_{ij}$, where the dimension of $i$ is given by the number of design parameters, $N$, referred to as *genes*, and the dimension of $j$ is given by the number of population members, $M$, referred to as *chromosomes*. An

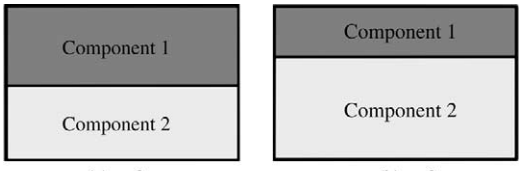


Fig. 4. Redundancy in sampling of the design space that results in identical bimaterial distributions.

objective function is chosen that mathematically describes the design performance objective. The objective function is evaluated for each chromosome to determine fitness. The two chromosomes that have the best fitness, $D_i^1$ and $D_i^2$, are then used to generate a new population of chromosomes, $D_{ij}^*$, using genetic concepts such as *crossover*, as follows:

$$D_{ij}^* = D_{ij}^1 A_{ij} + D_{ij}^2 B_{ij} \quad (\text{no sum};\ i = 1, \ldots, M,\ j = 1, \ldots, N), \tag{9}$$

where each chromosome of $D_{ij}^1$ and $D_{ij}^2$ are $D_i^1$ and $D_i^2$ respectively, while $A_{ij}$ and $B_{ij}$ are components of with values of either 0 or 1, and are governed by the property:

$$A_{ij} + B_{ij} = C_{ij}, \tag{10}$$

where $C_{ij}$ are components of a two-tensor whose values are all 1. To determine these values, a crossover value is first chosen. A matrix of random numbers is then generated with dimensions $i \times j$. If the value of the random number is above the crossover value, then the value of $A_{ij}$ will be 1, otherwise it is 0.

Another concept commonly used to generate new populations is *mutation*, as follows:

$$D_{ij}^* = D_{ij}^1 C_{ij} + \mu_{ij}(C_{ij} - 1) \quad (\text{no sum}), \tag{11}$$

where $C_{ij}$ is a matrix whose components are either 0 or 1, and $\mu_{ij}$ is a matrix of randomly generated values for a portion of the design variables. For this investigation, a GA incorporating the differential evolution (DE) strategy is employed instead of mutation because of its superior efficiency (Storn and Price, 1997). The DE strategy adds a differential step to the evolution process to generate a new population, $D_k^{\mathrm{DE}}$, as follows:

$$D_{ij}^{\mathrm{DE}} = D_{ij}^{1'} + F^*(D_{ij}^{2'} - D_{ij}^{3'}), \tag{12}$$

where $D_{ij}^{1'}$, $D_{ij}^{2'}$, and $D_{ij}^{3'}$ are populations that are generated by randomly rearranging the chromosomes in the current population, and $0 < F < 1$ is a weighting factor. Crossover can then be performed on each chromosome in the new population using the chromosome with the best fitness from the old population to evolve the next population. As the populations become optimal, the differences between chromosomes will become zero and the evolution of the populations will converge. A parametric study determined that for this design optimization problem, an initial population of 50, a value of 0.8 for the weighting factor, and a value of 0.7 for the crossover would produce the most efficient global convergence.

The GA proceeds through a number of evolved populations, known as *generations*, to determine the value of the design variables that optimizes the objective function. The best chromosome and the value of the objective function corresponding to this chromosome are recorded in each generation. According to the convergence criterion, convergence is attained when:

$$G_{i-\mathrm{numstop}}^{\mathrm{best}} - G_i^{\mathrm{best}} \leqslant \mathrm{tol}. \tag{13}$$

where $G_i^{\mathrm{best}}$ is the value of the objective function for the best chromosome in the $i$th generation, *tol* is the convergence tolerance, and 'numstop' is the number of generations over which the change in the objective function is less than the convergence tolerance. The choice of 'numstop' and 'tol' are critical for achieving good global convergence. The value of 'tol' will depend on the order of magnitude of the objective function and the order of the desired accuracy. For the convergence to be global, 'numstop' must be sufficiently large. If the value of this parameter is too small, then the optimum is most likely local. However, if the value of this parameter is too large, then the rate of convergence will slow down considerably. The parametric study determined that a value of 'numstop' equal to 1000 and a value of 'tol' equal to $10^{-8}$ were optimal.

The optimization of a composite structure using a GA typically occurs with no constraints on the material distribution, resulting in a large number of design variables. As was previously mentioned, the robust nature of the GA is more amenable to searching the multidimensional spaces generated by these design

variables than gradient-based techniques. However, optimizing with a one-dimensional gradient architecture constraint will greatly reduce the number of design variables. Therefore, the second reason for employing the GA over gradient techniques will no longer be applicable, rendering the modified formulation of the design problem more amenable to gradient-based techniques.

## 3. 3-D thermomechanical finite element simulation

The computational simulation used in this investigation consists of a 3-D thermomechanical, elasto-plastic finite element methodology that was previously developed and experimentally validated for optimizing thermal residual stress distributions graded nickel–alumina joints (Williamson et al., 1993; Rabin et al., 1998). The finite element simulation, as well as the design optimization problem, was solved on a Dell™ machine (512 MB RAM) with an Intel Pentium 3 Xeon™ processor (550 MHz). Continuum models were used to compute the deformations that develop in a metal-ceramic composite disk subjected to a 700 K thermal gradient through the thickness. Time-dependent material properties (i.e., creep phenomena) were not considered, because the temperatures were distributed in such a manner that they were below the creep temperatures for the associated microstructural distribution. The thermal boundary conditions would reasonably correspond to the situation expected for many thermal barrier coating applications.

The dimensions of the metal-ceramic composite disk are shown in Fig. 5. The diameter of the disk is 400 mm and the height is 120 mm. The disk consists of a composite material containing nickel (Ni) and alumina ($Al_2O_3$). A temperature of 1000 K is applied to the top surface and 300 K is applied to the bottom surface of the disk, while the edge of the disk is considered adiabatic (i.e., $dT/dn = 0$). Since the geometry and the boundary conditions are axisymmetric, an axisymmetric finite element model was used in the analysis. To simplify the modeling for the optimization problem, the disk was divided into layers of uniform composition through the thickness. This is also consistent with realistic material variations that have been achieved when manufacturing Ni–$Al_2O_3$ composite structures using powder processing technology (Rabin and Heaps, 1993). When a mesh was generated for the disk model, it was refined near the interface between the layers, as seen in Fig. 6.

Thermomechanical finite element simulations were performed with the Lagrangian ABAQUS computer code version 5.8 (Abaqus, 2000). The thermal behavior of the disk was assumed to be independent of the mechanical response, although the mechanical properties were thermally dependent. Therefore, the thermal distribution was initially determined, followed by the mechanical performance. All simulations utilized second order (quadratic) reduced integration elements. A separate program was used to calculate material properties corresponding to the composition of each element, as discussed in the following sections. For the

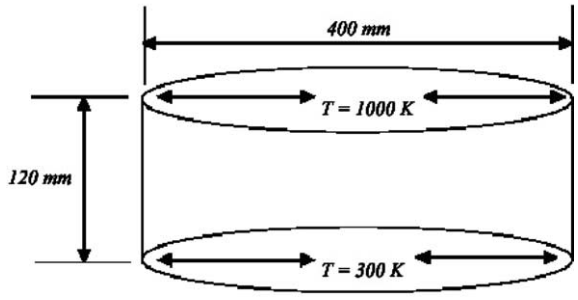


Fig. 5. Dimension of metal-ceramic composite disc subjected to 700 K thermal gradient in the design optimization problem.

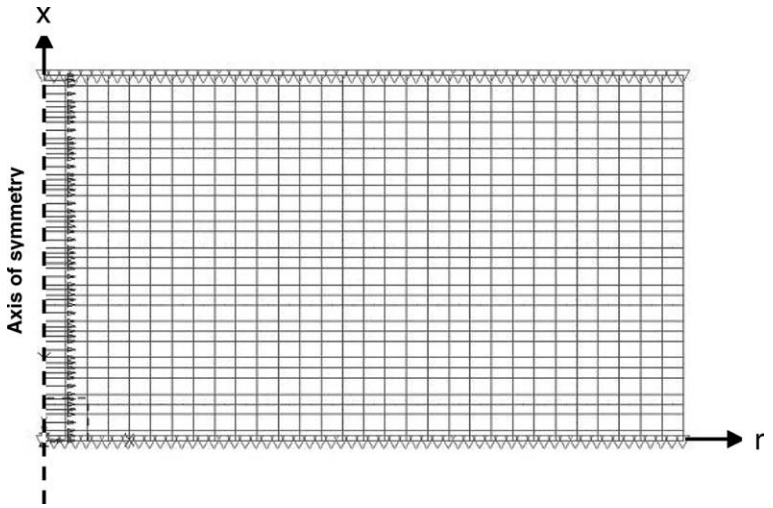


Fig. 6. Axisymmetric model of the metal-ceramic composite disk used in the finite element analysis with non-uniform element distributions in the $x$-direction related to the interfaces between layers of uniform composition.

elastic case, the average evaluation time was approximately 5 s for 1000 elements, while for the elastoplastic case it was approximately 160 s.

### 3.1. Constitutive material properties

For two-phase composites where one phase is discontinuous in a continuous matrix of the other phase, empirically adjusted combinations of rule-of-mixtures formulations are commonly employed to describe the experimentally observed stress–strain characteristics of the composite. A modified rule-of-mixtures formulation has been previously used to describe the elastoplastic behavior of two-phase metal-ceramic graded composites, and shown to be an accurate description for undamaged composites over wide volume fraction ranges (Williamson et al., 1993; Suresh and Mortenson, 1998; Bruck and Rabin, 1999a). In this formulation, the composite is treated as isotropic, with its uniaxial stress and strain given, respectively, by:

$$\sigma_c = f_1\sigma_1 + f_2\sigma_2, \tag{14a}$$

$$\varepsilon_c = f_1\varepsilon_1 + f_2\varepsilon_2, \tag{14b}$$

where subscripts 1 and 2 refer to the stresses, strains and volume concentrations of phases 1 and 2, respectively. The ratio of stress to strain transfer is then defined by the parameter, $q$, as follows:

$$q = \frac{\sigma_1 - \sigma_2}{\varepsilon_1 - \varepsilon_2}, \quad 0 < q < \infty, \tag{15}$$

where $q \to 0$ results in an isostress condition and $q \to \infty$ results in an isostrain condition. Combining Eqs. (14) and (15), one obtains:

$$E_c = \left\{ f_2\left(\frac{q+E_1}{q+E_2}\right) + f_1 \right\}^{-1} \left\{ f_2E_2\left(\frac{q+E_1}{q+E_2}\right) + f_1E_1 \right\}. \tag{16}$$

The specific choice of the empirical parameter $q$, depends widely on the internal constraints which arise from the particular spatial distribution of the phases in the composite the thermomechanical properties of the two phases and the residual stresses induced during processing.

The modified rule-of-mixtures formulation has also been extended to model elastopastic deformation of the two-phase composites. Fig. 7 schematically shows the determination of the uniaxial elastoplastic properties for a metal-ceramic composite using a bilinear representation of the elastoplastic deformation response of the constituents in the modified rule-of-mixtures formulation. Similar to the case of the elastic behavior, Eqs. (14)–(16), the effective plastic response of the composite is assessed by invoking the parameter $q$ in the following manner. The overall flow strength of the composite corresponding to the onset of plastic yielding, $\sigma_{yc}$, is given by:

$$\sigma_{yc} = \sigma_{y2} \cdot \left\{ f_2 + \left( \frac{q + E_2}{q + E_1} \right) \cdot \frac{E_1}{E_2} \cdot f_1 \right\}, \tag{17}$$

when the metal is continuous with yield strength, $\sigma_{y2}$. The strain hardening of the composite, described by the uniaxial tangent modulus, $H_c$, is:

$$H_c = \left\{ f_2 \left( \frac{q + E_1}{q + H_2} \right) + f_1 \right\}^{-1} \left\{ f_2 H_2 \left( \frac{q + E_1}{q + H_2} \right) + f_1 E_1 \right\}, \tag{18}$$

where $H_2$ is the instantaneous value of the elastoplastic tangent modulus of the metallic phase, as shown in Fig. 7. With the knowledge of the constitutive response of the individual phases and their volume fractions, the above formulations become complete. For the case of a graded composite, the variation of $f_1$ and $f_2$ with position needs to be provided.

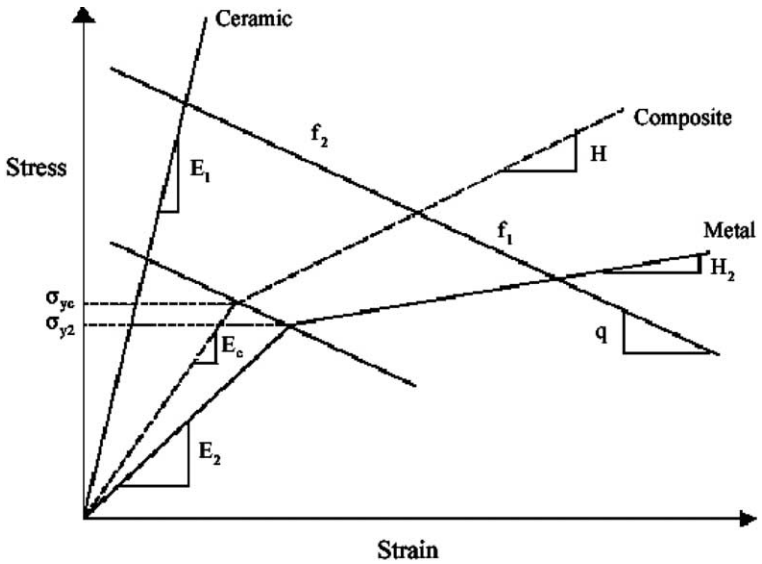


Fig. 7. Determination of uniaxial elastoplastic properties for a composite material using a bilinear representation of the elastoplastic deformation response of the constituents the modified rule-of-mixtures formulation.

### 3.2. Coefficient of thermal expansion and thermal conductivity

The coefficient of thermal expansion and thermal conductivity of the components are functions of the temperature. A linear rule-of-mixtures formulation is used to determine the effective coefficient of thermal expansion and thermal conductivity of the composite materials using the corresponding properties and volume fractions of the components (Williamson et al., 1993; Suresh and Mortenson, 1998):

$$\alpha_c = f_1\alpha_1 + f_2\alpha_2, \tag{19}$$

where $\alpha_c$ is the effective coefficient of thermal expansion of the composite material at a certain temperature and $\alpha_1$ and $\alpha_2$ are the coefficient of thermal expansion, at the same temperature, of components 1 and 2 respectively. In a similar manner, the effective thermal conductivity of the composite at a certain temperature, $k_c$ can be modeled as:

$$k_c = f_1k_1 + f_2k_2, \tag{20}$$

where $k_1$ and $k_2$ are the thermal conductivities, at the same temperature, of components 1 and 2 respectively. The thermal properties of undamaged metal-ceramic composites have been shown to be simply and reasonably described using these models over wide volume fraction ranges (Bruck and Rabin, 1999b).

## 4. Computational results

In this investigation, the thermal gradient will cause the composite structure to warp because of differences in thermal expansion between the hot front surface and cooler back surface. Therefore, computational results were obtained using an objective function that can be calculated easily and yields a very good approximation of the warping of the disk. This objective function is represented in terms of the nodal displacements for a typical out-of-plane displacement profile seen in Fig. 8 as follows:

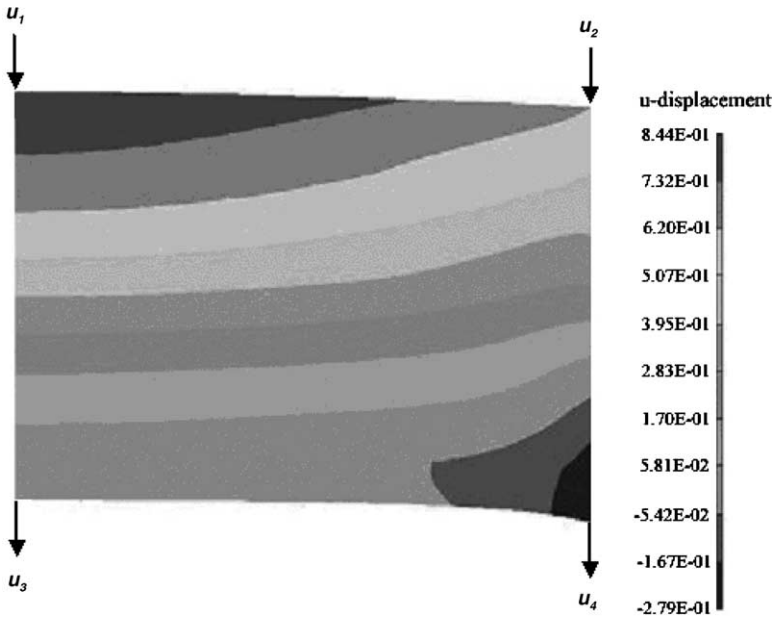


Fig. 8. Typical out-of-plane displacement profile associated with warpage of composite disk due to a thermal gradient.

$$G = u_1 - u_2, \tag{21}$$

where $u_1$ and $u_2$ are the displacements in the $x$-direction of the center node and edge node respectively on the hot surface of the disk. Because a computational analysis that use elastic material behavior is an order of magnitude faster than for elastoplastic material behavior and the elastic analysis can be used as a first-order approximation of the elastoplastic analysis for small scale yielding, simulations were conducted and compared for both of these cases.

### *4.1. Elastic analysis with no constraint on the material distribution*

The materials involved in the analysis are nickel and alumina. Alumina is a ceramic material. For all practical purposes, it can be assumed that alumina is perfectly elastic, while the nickel is a ductile metal. Nickel has a well-defined elastic and plastic deformation behavior, resulting in a non-linear material behavior that substantially increases the computational time for a finite element analysis. In the following case, nickel was assumed to be a perfectly elastic material in order to obtain faster numerical solutions. For this case, the disk was discretized into layers of homogeneous composition with no constraint placed on the material distribution through the thickness of the disk. Analyses were performed for 2, 3, 6, 10 and 30 layers, and the subsequent effects of the layer refinement on the optimal material distributions determined for each case can be seen in Fig. 9.

The $x$-axis of the graph represents the depth from the top surface and the $y$-axis represents the volume fraction of alumina present. It can be seen that the top layers are rich in alumina, a heat resistant material, and the bottom layers are rich in nickel, a strong and tough material. It can be seen that in the case of a disk with two layers, the top layer is fully alumina and the bottom layer is fully nickel. But as the number of layers increases, a trend can be observed, wherein for a few layers in between, the composition of alumina continuously reduces from unity to zero. Thus, the optimal material distribution more closely approaches a continuous gradient architecture as the number of layers is increased.

The predicted temperature distribution through the thickness of the disk with an optimal material distribution for 30 layers can be seen in Fig. 10. As expected, the temperature falls rapidly in the alumina

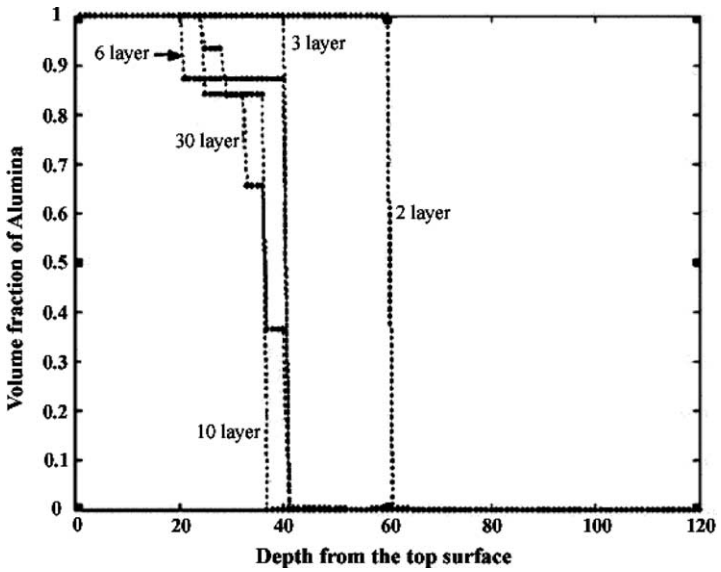


Fig. 9. The effects of layer refinement on the optimal material distribution in disk for the elastic case.

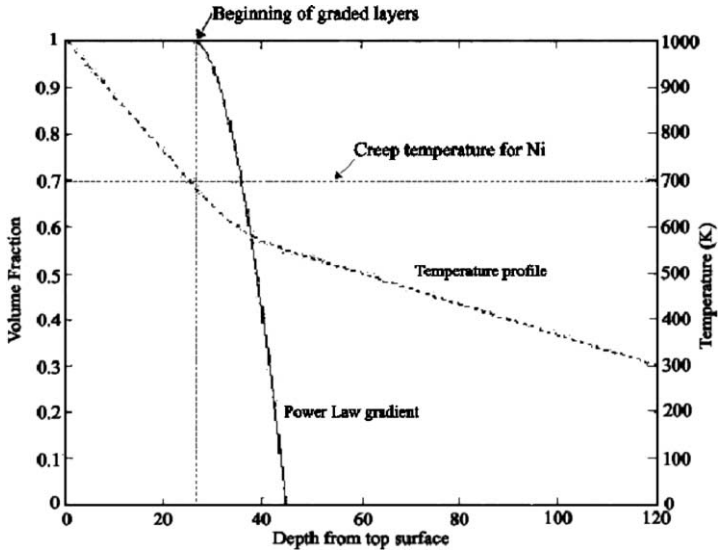


Fig. 10. Temperature and optimal material distribution through the thickness of a disk with 30 layers indicating the expected rapid decrease in temperature through the alumina and more gradual decrease through the nickel at levels below the creep temperature.

layers, then more gradually in the graded layers. The temperature at the beginning of the graded layers is 660 K. Previous studies have shown that for joints fabricated from nickel and alumina, creep strains in the metal regions can be neglected below 700 K, which is the creep temperature for nickel (Williamson et al., 1995). Therefore, the assumption that creep strains can be neglected appears to be valid for the optimal material distribution in the elastic case.

### 4.2. Elastoplastic analysis with no constraint on the material distribution

In this Analysis, nickel is modeled as a ductile material having well-defined elastic and plastic regions. Because of the computational complexity, only the 6 and 10 layers were analyzed by subdividing the disk into layers in the $x$-direction to determine the effects of layer refinement on the optimal material distribution. Fig. 11 shows the results obtained for these two cases. The optimal material distribution shows high concentration of alumina near the top, and a very gradual variation from alumina to nickel. But unlike the elastic case, the alumina concentration increases rapidly within 20 mm of the low temperature surface.

To explain the difference in the nature of the material distribution, the $x$ displacement profile of the disk is analyzed for the elastic and elastoplastic cases. Fig. 8 shows the displacement profile for the elastoplastic case. It can be seen that the displacement profile of the bottom surface of the disk is considerably different from that of the top surface, resulting in a higher concentration of alumina towards the bottom surface. This complex material distribution minimizes the distortions on the upper surface by shifting the distortions towards the bottom surface. A modified objective function was used as an alternative description of warping to mitigate these effects on the material distribution for the elastoplastic case.

### 4.3. Alternative description of the objective function

Results from the elastoplastic analysis indicate that the deformation of the top surface may not be a reasonable characterization of the warping of the disk along both the top and bottom surface. Therefore,

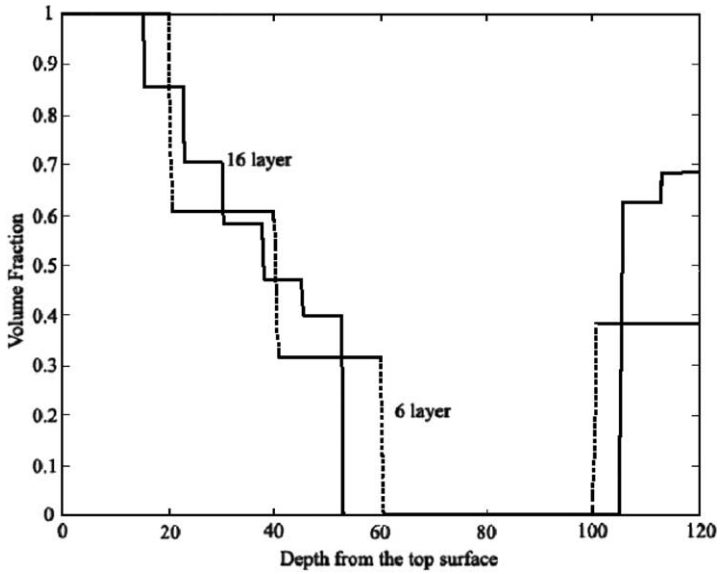


Fig. 11. The effects of layer refinement on the optimal material distribution in disk for elastoplastic case indicating a rapid increase in alumina concentration near the low temperature surface of the disk.

the objective function was re-structured to incorporate the deformation of the bottom surface as well. The modified objective function is, formulated as shown below.

$$G = u_1 - u_2 + u_3 - u_4, \tag{22}$$

where $u_1$, $u_2$, $u_3$ and $u_4$ are the displacements in $x$-direction of the center nodes and edge nodes on the hot and cold surfaces respectively, as shown in Fig. 8. This objective function was also used to determine the optimal material distribution in the disk, seen in Fig. 12. It can be seen that for the alternative description of the objective function, the gradient architecture is very similar to the elastic case.

### 4.4. Optimal material distribution using gradient architectures

The optimal material distribution in the previous cases was determined without constraining the nature of the material distribution in the structure in the thickness direction of the disk. The results indicate that the optimal material distribution will have a gradient architecture. Therefore, gradient architectures were applied as a constraint on the search space to determine the design parameters that minimize the given objective function. Initially, the optimization was conducted assuming a gradient architecture constraint with a one-dimensional power law description in Eq. (5). As was the case with no constraint on the material distribution, the model was discretized into a number of layers through the thickness of the disk. The composition of each layer was determined using the design parameters for the gradient architecture, generated by the optimization algorithm during each iterative step. The optimal design parameters obtained for different layering in the elastic case are shown in Table 1.

The optimal material distribution for the elastic case obtained for a 40-layered disk with and without using a gradient constraint on the material distribution is shown in Fig. 13. With 40 layers, the discrete layering begins to approach a continuous architecture represented by the gradient architecture constraint. The $x$-axis represents the depth from the top surface and the $y$-axis represents the volume fraction of alumina in the optimal material distribution. The material distributions are very similar in nature and their

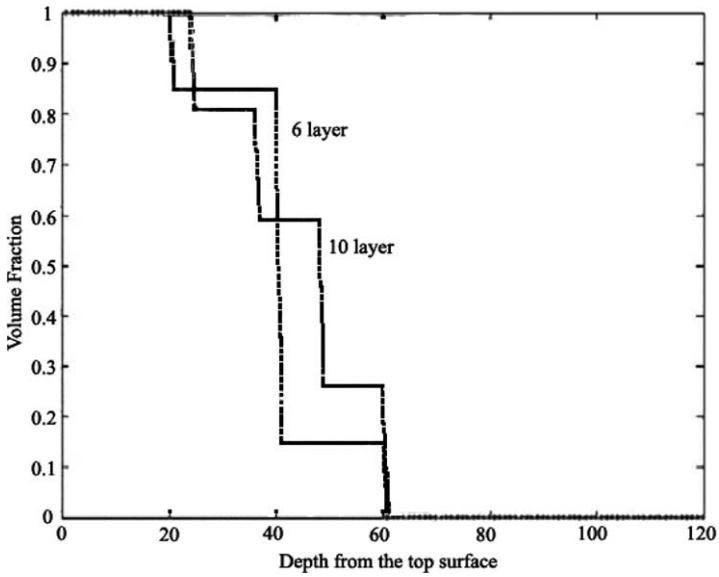


Fig. 12. Optimal material distribution in disk for elastioplastic case using alternative description of objective function exhibiting gradient architectures similar to the elastic case.

profiles almost overlap. However, only three design variables are required for the gradient architecture constraint, whereas for no constraints 40 design variables were required.

For the elastoplastic case, a single gradient is not adequate for describing the optimized material distribution. In this case, a multiple power law gradient architecture can be employed. This architecture is described as follows:

$$f_2 = \sum_{n=0}^{N} (-1)^n \left( \frac{x_n}{t_n} \right)^{p_n}, \tag{23}$$

where $N$ is the number of gradient architectures used to represent the material distribution. Eq. (23) now becomes the general basis for a new "material gradient optimization method" for composite structures. Using this optimization method, very complex material distributions can be described using fewer design variables. The optimized results for the generalized constraint description along with no constrain on the material distribution can be seen in Fig. 14, where only six design variables corresponding to $N = 2$ were used in the material gradient optimization method.

The correlation between the results using multiple gradient constraints and no constraint on the material distribution for the elastoplastic case is very similar to that observed in Fig. 13 when a single gradient constraint was used for the elastic case. However, the gradient is much steeper towards the cooler side of the disk. Since the analysis discretized the gradient architecture into layers, the associated layer composition for

Table 1
Optimal design parameters for the gradient architecture

| Number of layers | $x_0$ | $t$ | $p$ |
|---|---|---|---|
| 10 | 26.31 | 18.67 | 1.79 |
| 30 | 25.97 | 18.84 | 1.85 |
| 40 | 26.21 | 18.59 | 1.81 |

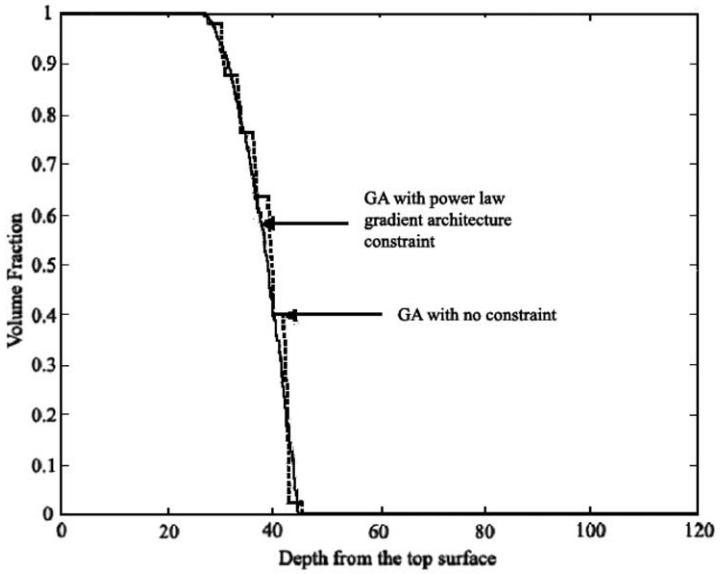


Fig. 13. Comparison of optimal material distributions for the pure GA without any gradient constraints and the GA with a power law gradient architecture constraint for the elastic case.

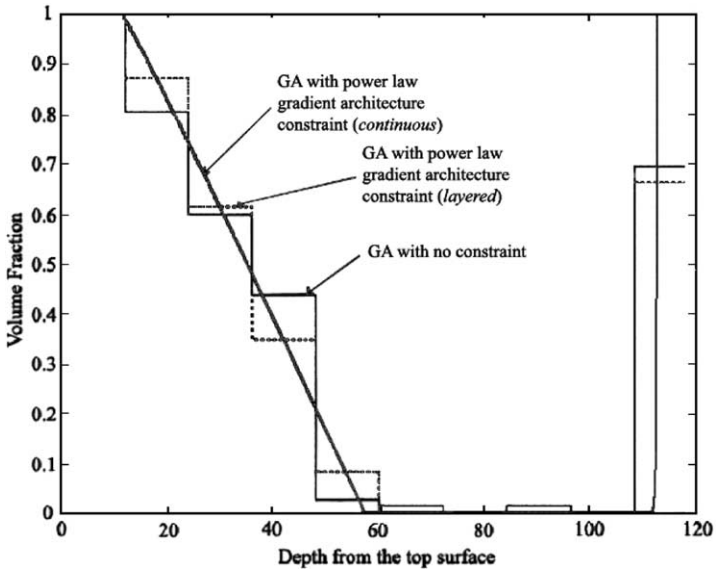


Fig. 14. Comparison of optimal material distributions for the pure GA without any gradient constraints and the GA with a power law gradient architecture constraint for the elastoplastic case.

the gradient architecture is also shown. The compositions are not exactly the same, which indicates that the global minimum for the elastoplastic case may not be well defined. Clearly, there could be more than one gradient that produces the same layer composition towards the end of the disk since the number of layers over which the gradient architecture extends does not exceed the number of design parameters used to

describe the composition gradient. Thus, the uniqueness of the optimal design parameters for the gradient architecture can depend upon the number of layers used in the finite element simulation. In general though, reasonable optimal solutions for coarser layering can exist despite the uniqueness of the design parameters.

## 5. Discussion

Results from the previous section show that both the optimization approaches yield the same optimal material distribution. However, the two approaches can be differentiated by comparing the computational time consumed by the GA in each approach. The majority of the total time taken for the algorithm to converge is occupied by the execution of the finite element simulations. Evaluation of the objective function corresponding to a population member results in the execution of the finite element routine once. So a measure of the number of objective functions evaluated before achieving convergence will be a good measure of the efficiency of the algorithm. Fig. 15 indicates the variation of the value of the objective function for the GA with the number of function evaluations, using a population set of 40. The $x$-axis represents the number of objective function evaluations and the $y$-axis represents the value of the objective function.

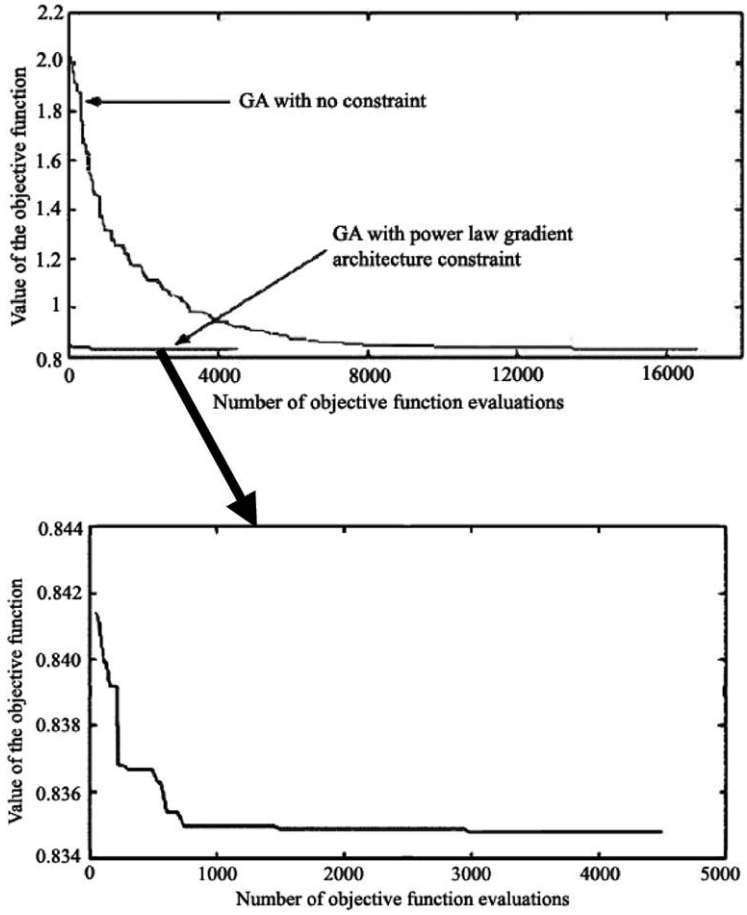


Fig. 15. The comparison of convergence rates for the GA with and without a gradient architecture constraint for the elastic case indicating much faster convergence when the constraint is used.

It can be seen from the graph that the number of function evaluations taken for convergence of the algorithm using a gradient architecture constraint is significantly lower than the algorithm with no constraint on the material distribution. A magnified graph describing the convergence of the algorithm using a gradient architecture constraint can also be seen in Fig. 14. In this graph, the starting point for the optimization routine is very close to the optimum (within 1%, opposed to 115–130% when there are no constraints on the material distribution), thereby indicating that the gradient architecture enhances the performance of the algorithm by substantially increasing the convergence rate. Not only does the gradient architecture only require three design variables as opposed to more than 3 when no constraint on the material distribution is used, but as mentioned previously, gradient architectures naturally optimize the performance of structures (Kreuz et al., 2001; Amada et al., 1997).

GAs make use of a stochastic global search strategy to find the optimum. The randomness of these algorithms suggests that the nature of variation of the value of the objective function over the course of iterations need not be the same for different runs of the same optimization problem. To obtain an idea about the nature of convergence, the same problem is optimized a number of times, and the results are compared. Figs. 16 and 17 describe the variation of convergence rate for the GA with and without the gradient architecture constraint in the elastic case.

The convergence rate is similar for different runs of the same problem with or without the gradient architecture constraint. The initial population set is randomly constructed from the domain constraints. The values of the objective function corresponding to the best population member of the initial population set are close to each other. The algorithm converges to the optimum quickly, but it takes a considerably longer time to obtain near absolute convergence.

In the case of optimization with no constraint on the material distribution, the number of design variables increase as the number of material groups is increased. But in the case of optimization with a gradient architecture constraint, the number of design variables is constant, and equals three. Table 2 shows the number of objective function evaluations taken for these two cases, when the number of layers was increased. $G_{\text{start}}$, $G_{\text{optimum}}$ and $N_{\text{conv}}$ represent the best value of the objective function in the initial parent

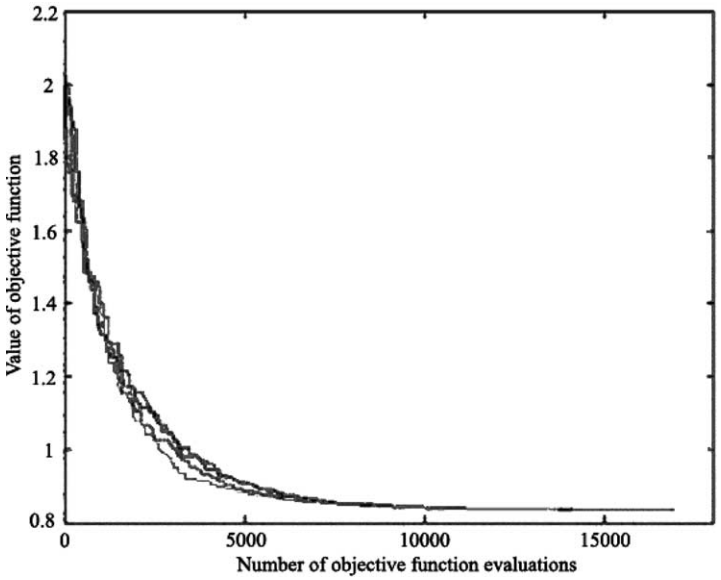


Fig. 16. Variation of convergence rate for GA with no constraint on the material distribution in the elastic case.

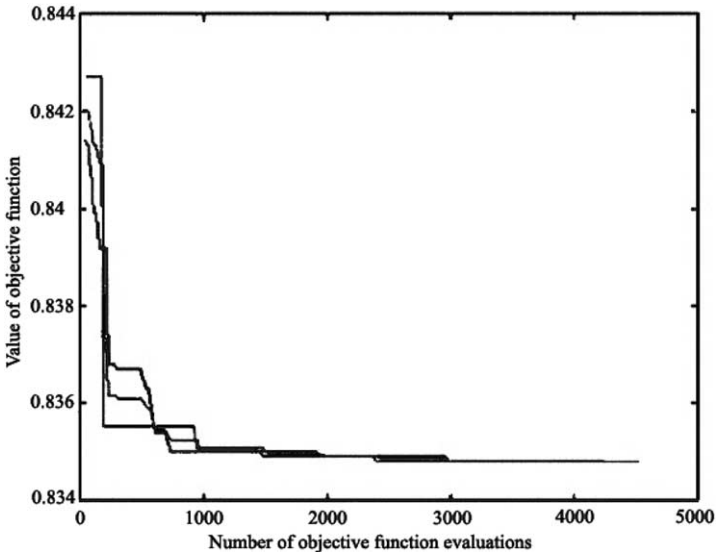


Fig. 17. Variation of the convergence rate for the GA with a gradient architecture constraint in the elastic case.

Table 2
Comparison of convergence rates, $N_{conv}$, with initial and optimum objective function values, $G_{init}$ and $G_{optimum}$, for conventional homogenization method and modified formulation using gradient architecture

| Number of layers | Conventional homogenization method | | | Modified formulation using 1-D gradient architecture | | |
|---|---|---|---|---|---|---|
| | $G_{init}$ | $G_{optimum}$ | $N_{conv}$ | $G_{init}$ | $G_{optimum}$ | $N_{conv}$ |
| 10 | 1.6415 | 0.8349 | 13017 | 0.8728 | 0.8350 | 4639 |
| 30 | 1.7652 | 0.8351 | 17214 | 0.8512 | 0.8348 | 4558 |
| 40 | 2.0268 | 0.8350 | 18978 | 0.8414 | 0.8349 | 4510 |

population, the value of the objective function corresponding to the optimal material distribution and the number of evaluations of the objective function before achieving the convergence respectively. When no constraint is placed on the nature of the optimal material distribution, the number of objective function evaluations needed to attain convergence increases as the number of layers in the disk is increased. This can be attributed to the increased randomness in the design search space that is associated with the increase in the number of material groups. In contrast, introducing a gradient architecture constraint slightly reduces the number of objective function evaluations required to obtain convergence as the number of layers is increased. This can be attributed to a more clearly defined minimum in the design search space associated with the improved continuity of the material distribution when the number of layers is increased. The comparison of these two design optimization approaches clearly indicates that the gradient architecture constraint approach is more efficient in obtaining the material distribution.

For the elastoplastic case, the convergence rates for the multiple power law gradient architectural constraint is compared with no material constraint in Fig. 18. Similar to the single gradient constraint for the elastic case, the value of the objective function for the multiple gradient architecture constraint for the elastoplastic case is initially closer to the optimum (within 50%), while for no material constraint it is nearly 300% greater. Although the gradient appears to converge after 500 function evaluations, approximately 2000 function evaluations are required for absolute convergence. After 6000 function evaluations, no

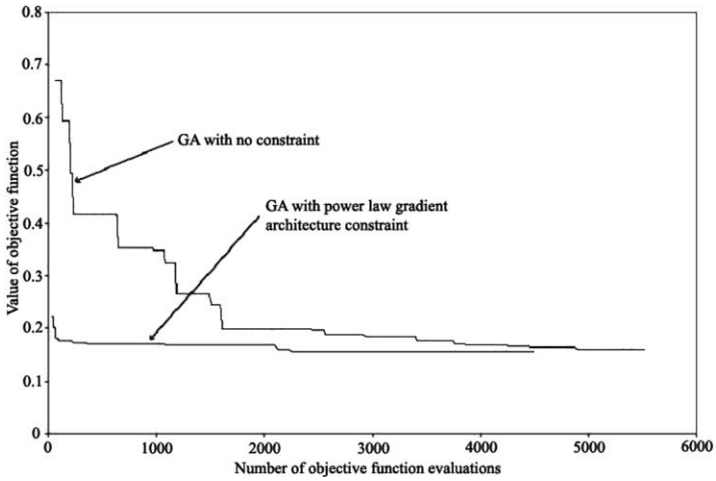


Fig. 18. Comparison of convergence rates for GA with and without the multiple power law gradient architectural constraint in the elastoplastic case.

constraint on the material distribution is only 0.6% greater than the multiple gradient constraint (0.1572 as opposed to 0.1563). The differences in the objective function can be attributed to the differences observed in the layer compositions in Fig. 14, and indicates that the global optimum for the elastoplastic case will not necessarily be well defined.

It is also important to note that the composite structures optimized using the gradient architecture constraint consist of two-phase composites exhibiting isotropic properties that are accurately predicted from knowledge of their composition using the rule-of-mixtures formulations described in Sections 3.1 and 3.2. Optimization of composite structures consisting of materials that exhibit either anisotropic or transversely isotropic properties, such as fiber-reinforced composites, would require knowledge not only of their composition gradient, but the variation in their material anisotropy as well. Since the composition gradients described in Eqs. (5) and (23) would no longer be adequate to describe the material distribution in the composite structure, the material anisotropy of each element would have to be included as additional design variables with associated constraints in the design optimization problem. The effects of adding design variables to account for material anisotropy in the optimization of composite structures would require further investigation in order to determine the exact benefits derived from using gradient architecture constraints on the material distributions in these structures.

## 6. Conclusions

A systematic investigation into the enhancement of GAs for optimizing the material distribution in composite structures using gradient architectures was conducted. A design optimization problem was formulated to find the material distribution in a composite structure that results in the optimized performance of the structure under a given set of operating conditions. The formulation combines the powerful and efficient performance of a DE GA optimization technique with 3-D thermomechanical finite element simulations of structural performance that are capable of handling the non-linearity in composite material behavior, as well as arbitrary thermomechanical boundary conditions. To enhance the computational efficiency of the GA in the design optimization problem, the formulation of the problem was modified using a

gradient architecture to reduce the number of design variables and constrain the design search space. To demonstrate the improvement in computational efficiency, distortions in a disk subjected to a thermal gradient were minimized.

A comparison of the time taken for the optimization routine using no constraints on the material distribution and the formulation of the problem constrained with a gradient architecture indicated that employing gradient architecture concepts reduce the computational time for absolute convergence anywhere from 70–80%, due to the reduction in the number of design variables and the natural optimization provided by a gradient architecture. Objective functions were also found to be substantially closer to the minimum using the gradient architecture constraint, and within 1% of the minimum for the elastic case. As the number of layers used to define the gradient is increased, the convergence improved slightly with the gradient architecture constraint whereas it increased when no constraint is employed. Thus, it has been shown that by placing a gradient architecture constraint on the nature of the material distribution, the computational time can be significantly reduced for the design optimization of composite structures. Reducing the number of design variables using the gradient architecture constraint will also render the design problem more amenable to gradient-based optimization methods.

For the elastoplastic case, the optimal material distribution can be more complex than for the elastic case, depending upon the choice of objective function. A generalized "material gradient optimization method" has been proposed that significantly reduces the number of design variables for composite structures. Using this method, the difference between the constrained and unconstrained optimization results were similar to those observed using the single gradient constraint for the elastic case. However, absolute convergence was achieved after 2000 instead of 500 function evaluations. It was also observed that the optimal objective function value for no constraint on the material distribution was 0.6% greater than for the gradient architecture, and there were slight differences between the optimal layer compositions. This indicated that the global optimum for the elastoplastic case was not well defined. Furthermore, it was noted that the gradient architecture will not be unique if the number of layers over which the gradient architecture extends is less than the number of design parameters used to describe the composition gradient in the finite element simulation.

## Acknowledgements

This work was sponsored by Dr. James Short under Office of Naval Research award number N000140010472, and by Dr. Bruce LaMattina under Army Research Office award number DAAD190210343.

## References

Amada, S., Ichikawa, Y., Munekata, T., Nagese, Y., Shimizu, H., 1997. Fiber texture and mechanical graded structure of bamboo. Composites Part B 28B, 13–20.

Bendsoe, M.P., Kikuchi, N., 1988. Generating optimal topologies in structural design using homogenization method. Computer Methods in Applied Mechanics and Engineering 71, 197–224.

Bever, M.B., Duwez, P.E., 1972. Gradients in composite materials. Material Science and Engineering 10, 1–8.

Bruck, H.A., Rabin, B.H., 1999a. Evaluating microstructural and damage effects in rule-of-mixtures predictions of the mechanical properties of Ni–$Al_2O_3$ composites for use in modeling functionally graded materials. Journal of Materials Science 34, 2241–2251.

Bruck, H.A., Rabin, B.H., 1999b. An evaluation of rule-of-mixtures predictions of thermal expansion in powder processed Ni–$Al_2O_3$ composites. Journal of the American Ceramic Society 82, 2927–2930.

Finot, M., Suresh, S., Glannakopoulos, A.E., 1994. Sharp interfaces versus functionally graded metal-ceramic layers: geometrical optimization for mechanical response. In: Proceedings of the third International Symposium on Structural and Functional Gradient Materials, pp. 720–731.

Goettler, R.W., Kelly, J.T., Wagner, R.A., 1997. Ceramic composites technology development for industrial applications. Proceedings of ASME Mechanical Engineering Congress and Exposition on Composites and Functionally Graded Materials 80, 341–347.

Kreuz, P., Arnold, W., Kesel, A.B., 2001. Acoustic microscopic analysis of the biological structure of insect wing membranes with emphasis on their waxy surface. Annals of Biomedical Engineering 29, 1054–1058.

Markworth, A.J., Ramesh, K.S., Parks Jr., W.P., 1995. Review: modelling studies applied to functionally graded materials. Journal of Materials Science 30, 2183–2193.

Nadeau, J.C., Ferrari, M., 1999. Microstructural optimization of a functionally graded transversely isotropic layer. Mechanics of Materials 31, 637–651.

Niino, M., Maeda, S., 1990. Recent development status of functionally gradient materials. ISIJ International 30, 699–703.

Ootao, Y., Tanigawa, Y., Ishimaru, O., 1999. Optimization of material composition of functionally graded plate for thermal stress relaxation using a genetic algorithm. Journal of Thermal Stresses 23, 257–271.

Rabin, B.H., Heaps, R.J., 1993. Powder processing of Ni–$Al_2O_3$ FGM. Ceramic Transactions 34, 173–180.

Rabin, B.H., Williamson, R.L., Bruck, H.A., Wang, X.L., Watkins, T.R., Clarke, D.R., 1998. Residual strains in an $Al_2O_3$–Ni joint bonded with a composite interlayer: experimental measurements and FEM analysis. Journal of the American Ceramic Society 81, 1541–1549.

Sadagopan, D., Pitchumani, R., 1998. Application of genetic algorithms to optimal tailoring of composite materials. Composites Science and Technology 58, 571–589.

Shimojima, K., Yamada, Y., Mabuchi, M., Saito, N., Nakanishi, M., 1999. Optimization method of FGM compositional distribution profile design by genetic algorithm. Materials Science Forum 308, 1006–1011.

Storn, R., Price, K., 1997. Differential evolution—a simple and efficient heuristic for global optimization over continuous spaces. Journal of Global Optimization, Kluwer Academic Publishers 11, 341–359.

Suresh, S., Mortenson, A., 1998. Fundamentals of Functionally Graded Materials. Institute of Materials, London, UK.

Swan, C.C., Kosaka, I., 1997. Homogenization-based analysis and design of composites. Computers and Structures 64, 603–621.

Takaka, K., Tanaka, Y., Enomoto, K., Poterasu, V.F., Sugano, Y., 1993. Reduction of thermal stresses in functionally graded materials. Computer Methods in Applied Mechanics and Engineering 106, 271–284.

Takano, N., Zako, M., Nakagawa, M., Takeda, N., 1998. Design of microstructures for the emergence of macroscopic function by homogenization method and genetic algorithms. Materials Science Research International 4, 153–158.

Williamson, R.L., Rabin, B.H., Byerly, G.E., 1995. FEM study of the effects of interlayers and creep in reducing residual stresses and strains in ceramic-metal joints. Composites Engineering 5, 851–863.

Williamson, R.L., Rabin, B.H., Drake, J.T., 1993. Finite element analysis of thermal residual stresses at graded ceramic-metal interfaces. Part I. Model description and geometrical effects. Journal of Applied Physics 74, 1310–1320.